ORIGINAL ARTICLE

Hydrochemical and geoelectrical investigation of Marine Jeffara Aquifer, southeastern Tunisia

Belgacem Agoubi · Adel Kharroubi · Tarek Abichou · Habib Abida

Abstract Hydrogeochemical and geophysical investigation were carried out to assess the geochemical water composition and processes governing groundwater hydrochemistry in Marine Jeffara Aquifer, southeastern Tunisia. A total of 74 groundwater samples were collected and analyzed for various parameters such as pH, electrical conductivity and major ions. Statistical and geochemical modeling were performed to understand the processes controlling groundwater geochemistry. According to their dominance, major ions are classified as follows $Cl > Na > SO_4 > Ca > Mg > HCO_3$. Hydrochemical, $Na–Ca–Cl–SO_4$, $Ca–Na–Mg–Cl–SO_4$ and $Mg–Ca–Cl–SO_4$ are the dominant forms in groundwater, mainly as a result of rock–water interaction and saltwater intrusion. Ten vertical electrical resistivity tests were performed in three profiles. The measured low values of electrical resistivity in the coastal areas indicate saltwater mixing with groundwater, as a result of saltwater intrusion.

Introduction

The freshwater crisis is already felt in arid and semi-arid areas like the Marine Jeffara region in southeastern Tunisia on the Mediterranean sea. This region is facing increasing freshwater needs due to a rapidly growing population and increased urbanization. Faced with the scarcity of surface water, fresh groundwater is the main source of water supply. Rapid increase of salinity is the most widespread form of Marine Jeffara groundwater contamination. This is manifested in an increase of total dissolved solids (TDS) and some specific chemical constituents such as Cl, Na, Ca, Mg, and SO_4 (Geminez and Morell 1997; Reddy et al. 2010).

Although groundwater quality changes along the course of movement of water through the hydrological cycle, several natural and anthropogenic processes may contribute to groundwater mineralization (Thilagavathi 2012). Some examples are rock–water interaction, mineral dissolution, agriculture and industrial effluents, mixing water, cation exchange and saltwater intrusion (Appelo and Postma 2005; Reddy et al. 2010; Thilagavathi 2012). High mineralization levels are typically due to recurrent farming and excessive pumping, in turn causing deterioration in groundwater quality and saltwater intrusion (Pazand and Hezarkhani 2012; Bear et al. 1999; Mahesha and Nagaraja 1996).

Numerous studies undertaken in arid and semi-arid coastal areas have included hydrochemical analysis. More specifically, hydrochemical composition and ionic ratios were used to identify the origin of groundwater mineralization processes and saltwater intrusion in coastal areas (Bear et al. 1999; Djabri et al. 2008; Reddy et al. 2010;

B. Agoubi (✉) · A. Kharroubi
UR: Applied Hydro-Sciencces, Higher Institute of Water Sciences and Techniques, University of Gabes, Gabes, Tunisia
e-mail: Belgacem.Agoubi@isstegb.rnu.tn

A. Kharroubi
e-mail: Adel.Kharroubi@isstegb.rnu.tn

T. Abichou
Department of Civil and Environmental Engineering, Florida State University, 2525 Pottsdamer street, Tallahassee, FL 32311, USA
e-mail: tarek.abichou@gmail.com; abichou@eng.fsu.edu
URL: www.eng.fsu.edu/~abichou

H. Abida
Department of Earth Sciences, Faculty of Sciences, University of Sfax, Sfax 4000, Tunisia
e-mail: Habib.Abida@fss.rnu.tn

Fig. 1 Geological map and
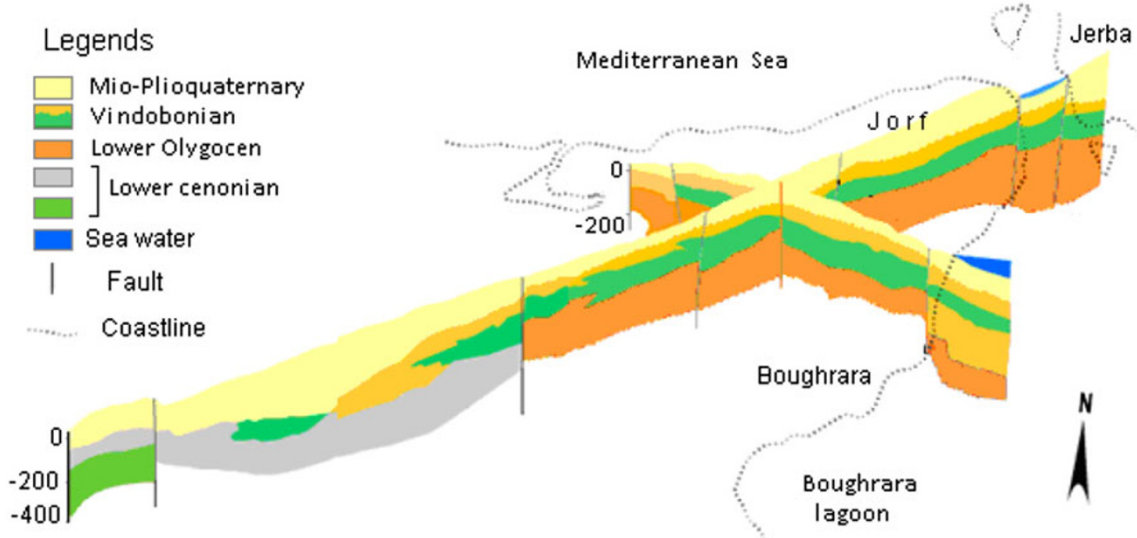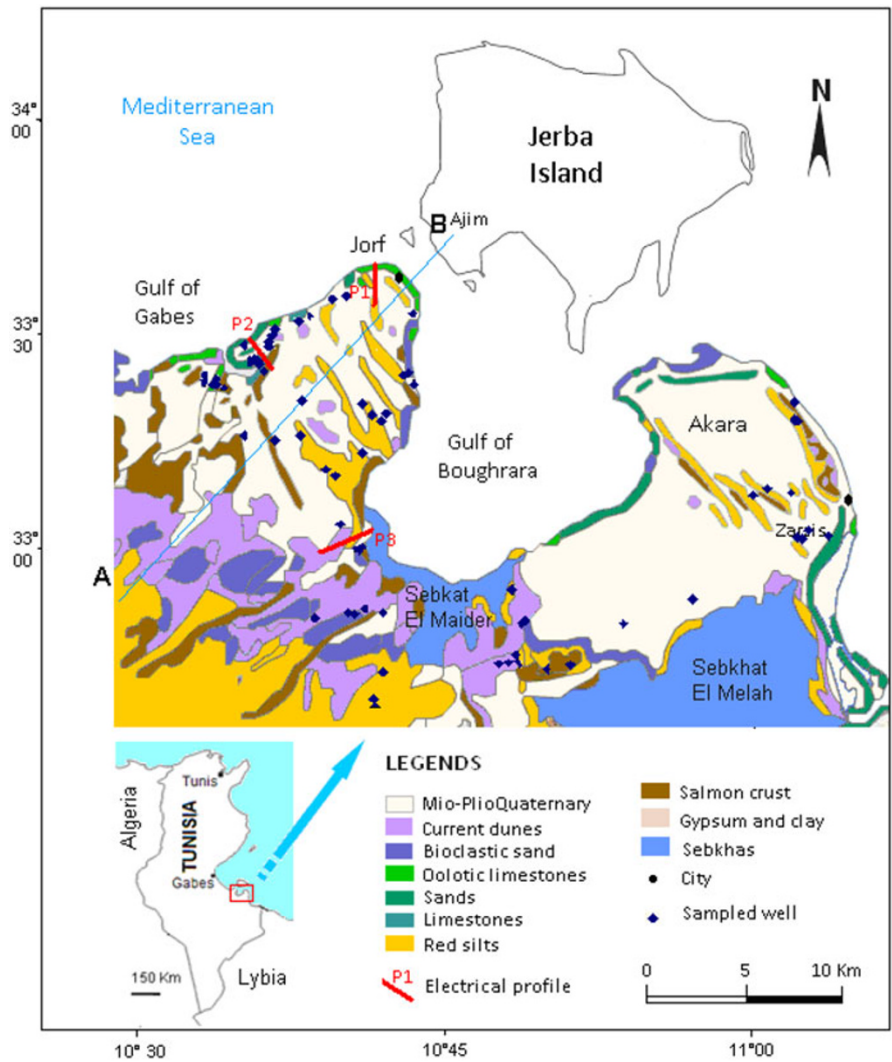location of study area (Afer,
Jedoui 2000)

Fig. 2 Geological and hydrogeological cross-section **a**, **b** (Afer, Mekrazi 1974, modified)

Table 1 Analytical results of groundwater samples from marine Jeffara

Well nb.	Coordinates						Mesure in situ		TDS (g/l)	Major ions (Meq/l)						
	X			Y			CE ms/cm 25 °C	pH								
	D	M	S	D	M	S				Ca	Mg	Na	K	SO$_4$	Cl	HCO$_3$
1	33	37	8	10	34	57	6.1	7.56	5.36	35.2	13.8	24	0.58	38	32	4
2	33	37	17	10	34	35	6.01	7.82	5.2	29.6	16	26.4	0.7	38.5	27	3.3
3	33	37	15	10	34	30	6.34	7.34	5.64	24	22.4	23.05	0.62	35.5	33	7.15
4	33	37	19	10	34	38	7.91	7.76	6.44	36	13.6	44.5	0.78	44	42	6.9
5	33	37	18	10	34	26	9.68	7.66	9.08	44.8	18.4	44	0.68	27	75	4.2
6	33	37	27	10	33	57	7.08	7.72	6.24	35.2	15.2	34	0.54	46	42	2.6
7	33	37	47	10	34	4	6.96	7.77	5.88	28	20.8	36	0.45	50	39	2.6
8	33	38	22	10	36	33	3.94	7.76	3.64	24	16	12.2	0.41	36	14	3
9	33	38	25	10	36	30	6.36	7.68	5.16	25.6	16.4	29.4	0.5	33	33	3.35
10	33	38	25	10	36	25	8.48	7.65	7.16	31.2	19.2	45.5	0.67	31	54	7.25
11	33	38	21	10	36	13	9.75	7.56	8.44	28.8	31.2	52	0.72	48.5	65	3.7
12	33	38	20	10	36	11	10.8	7.64	8.84	28.8	30.4	62	0.8	42	74	2.75
13	33	38	15	10	36	39	3.63	7.73	3.4	11.2	26.4	9.8	0.37	39	10	3.7
14	33	39	3	10	37	2	5.17	7.6	4.8	14.4	32.8	17.6	0.49	31	26	5.75
15	33	38	52	10	37	21	5.68	7.63	4.96	26.4	18.6	22.6	0.48	30.5	30	4
16	33	39	15	10	37	4	6.15	7.63	5.36	26.4	20	26	0.51	30.5	30	4
17	33	39	29	10	37	11	5.98	7.66	5.04	18.4	25.6	27.2	0.44	31	32	5.4
18	33	39	39	10	37	22	5.58	7.67	5.28	35.2	12	20	0.43	26	30	6.45
19	33	40	11	10	38	24	8.84	7.66	7.56	33.6	21.6	46	0.75	32	60	0.85
20	33	40	26	10	38	59	10.16	7.67	8.44	26.4	33.6	60.5	0.42	36	71	5.3
21	33	40	31	10	38	57	13.11	7.66	11.28	51.6	22.8	71.5	0.9	45.5	104	3.5
22	33	41	10	10	40	4	5.76	7.74	5.16	37.2	11.6	22.6	0.48	39.5	36	3.1
23	33	41	16	10	40	43	6.91	7.44	6.24	40.4	10.8	35	0.52	41	48	2.6
24	33	40	28	10	43	42	16.88	7.66	13.48	45.2	35.6	104.5	1.6	55	142	5.2
25	33	37	56	10	43	15	7.18	7.7	6.2	34.4	15.2	37	0.64	40.5	52	2.1
26	33	37	44	10	43	28	6.91	7.67	5.84	34.4	10.4	25.6	0.58	35	40	2.7
27	33	37	10	10	43	10	5.85	7.77	4.6	34.4	10.4	25.6	0.58	35	40	2.7
28	33	34	54	10	35	48	8.95	7.71	6.96	25.6	25.6	52.75	0.83	45	52	2
29	33	34	52	10	35	50	6.2	7.76	5.2	28	17.6	27	0.58	40	29	2.5
30	33	34	39	10	37	14	10.57	6.65	9.2	3.2	56	51	2.38	45	70	1.95
31	33	33	50	10	38	21	4.9	7.42	4.16	8	29.6	21.2	0.52	38.5	18	4.45
32	33	33	18	10	39	39	4.63	7.51	4.2	10.4	32.8	14.6	0.5	29.5	20	4.1
33	33	33	0	10	40	4	6.34	7.59	5.48	3.2	39.2	25	0.52	31.5	36	3.05
34	33	34	5	10	41	15	5.62	7.68	4.84	25.6	18.4	22.2	0.59	34.5	26	1.55
35	33	35	34	10	42	13	7.06	7.57	5.68	28.8	19.2	38	0.57	50	39	1.5
36	33	35	54	10	42	25	6	7.59	5.4	36.8	12.8	20.6	0.59	32.5	33	1.9
37	33	35	48	10	41	48	6.49	7.54	5.48	26.4	18.4	33	0.56	36.5	36	1.55
38	33	33	36	20	41	16	5.1	7.52	4.48	26.4	16.8	18.2	0.47	33	23	1.6
39	33	30	45	10	40	11	10.05	7.61	7.76	16	33.6	59.5	0.7	36	66	2
40	33	29	42	10	41	11	11.75	7.75	9.48	20	44.8	68	0.64	54.5	74	2.35
41	33	29	38	10	41	2	13.21	7.66	10.32	21.6	43.2	80	1.03	56	90	2.1
42	33	29	33	10	41	2	10.46	7.62	8.48	16	38.4	59	0.74	45	75	1.9
43	33	29	37	10	40	55	10.8	7.72	8.44	24	32.8	62.5	0.86	46.5	76	2.5
44	33	26	39	10	42	7	6.6	7.73	5.36	11.2	27.8	38	0.61	30	38	2.15
45	33	26	48	10	41	15	5.52	7.78	4.08	7.2	25.8	36	0.5	35.5	28	1.85
46	33	26	35	10	40	45	5.71	7.78	4.24	6.4	26.4	32.6	0.52	28.5	32	2
47	33	26	37	10	40	27	5.89	7.75	4.56	9.6	22.4	36.25	0.51	42.5	30	2
48	33	26	26	10	39	3	7.85	7.9	6.32	27.6	23.6	48.5	0.66	47	42	2.9
49	33	23	54	10	42	4	24.2	7.7	18.84	24.8	60	162	1.6	71	198	6.6
50	33	22	40	10	41	40	6.13	7.91	4.72	12	24	32.4	0.6	29.5	33	3.65
51	33	22	18	10	41	42	5.35	7.84	3.88	8.8	25.2	29.4	0.57	24.2	30	4.85
52	33	24	10	10	10	47	8.75	7.6	7.4	31.2	32.8	43	0.67	54	58	4.4

Table 1 continued

| Well nb.	Coordinates						Mesure in situ		TDS (g/l)	Major ions (Meq/l)						
	X			Y			CE ms/cm 25 °C	pH		Ca	Mg	Na	K	SO₄	Cl	HCO₃
	D	M	S	D	M	S										
53	33	24	15	10	47	53	9.02	7.66	7.48	30.8	31.2	44.5	0.59	56.5	60	1.6
54	33	24	37	10	48	12	7.43	7.8	6.24	27.2	30	36.5	0.71	59	42	1
55	33	25	12	10	48	24	7.19	7.73	6.12	22.4	34.8	35.5	0.7	45	39	2.75
56	33	25	18	10	48	17	7.4	7.76	6.2	28	26.8	36.5	0.6	42	43	3.05
57	33	26	2	10	48	33	10.68	7.63	8.36	26.8	27.4	61	0.96	49	68	4.71
58	33	26	8	10	48	41	9.43	7.59	7.56	31.2	21.6	51.5	0.77	45.5	58	3.35
59	33	26	8	10	48	42	9.42	7.63	7.64	25.2	28.4	52.5	0.95	54.5	56	3.3
60	33	27	37	10	48	6	7.21	7.67	6.12	26.4	28.4	39	0.85	57	35	3.9
61	33	23	55	10	49	37	7.3	7.79	6.16	27.2	33.8	36	0.66	55.5	43	2.35
62	33	24	7	10	50	45	10.65	7.71	8.8	27.2	44.8	53	0.98	55	47	3.55
63	33	25	58	10	53	17	10.27	7.57	8.52	32	41	47.5	0.9	48	72	3.55
64	33	32	8	11	0	3	9.56	7.69	6.88	10.4	35.2	53.5	0.78	21	80	2.5
65	33	31	50	10	59	24	8.09	7.78	5.92	8.4	27.2	51	0.8	29.5	58	3.5
66	33	35	15	11	1	32	8.17	7.59	6.4	27	18.8	40	0.95	25.5	59	2.6
67	33	27	8	10	56	29	13.84	7.59	10.76	31.6	38.8	80	1.09	60	104	2.1
68	33	29	51	11	2	49	7.13	6.98	5.12	8	6.4	55	1.82	0.8	70	3.6
69	33	30	6	11	1	54	6.94	7.65	5.08	16.8	11.2	45.5	0.54	16.4	60	1.7
70	33	29	45	11	1	40	7.7	7.66	5.88	19.2	16.8	47.5	0.58	21	72	1.8
71	33	29	49	11	1	25	5.68	7.78	4	11.2	10.4	32.8	0.52	12	38	1.9
72	33	36	5	11	1	25	6.42	7.78	4.72	18.4	16	38.5	0.85	17.5	55	8.4
73	33	35	22	11	1	25	10.95	7.51	8.96	40.8	21.6	58.5	4.6	35.5	82	6.6
74	33	31	53	11	1	8	5.81	7.68	4.48	12.8	15.2	31.8	0.55	11.6	48	2.7

Fig. 3 Piper diagram describing groundwater quality
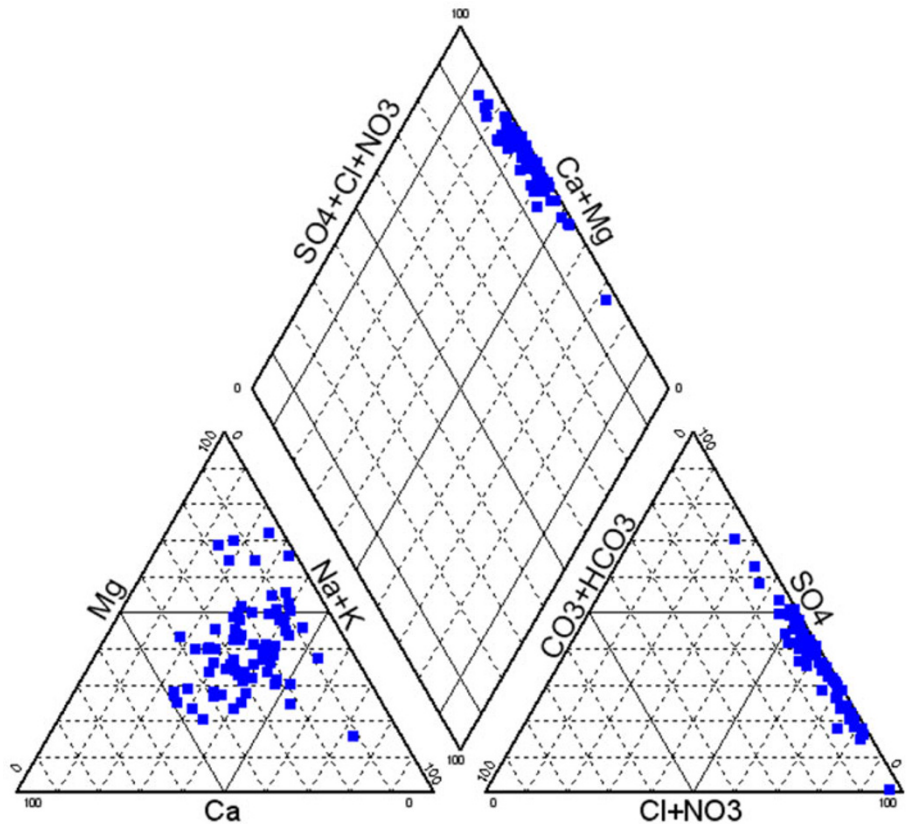
Table 2 Chemical facies of groundwater from marine Jeffara

Water type	Water percentage		Chemical facies (%)
Ca–Mg–Cl–SO$_4$	1.3	22	Chlorinated calcium and magnesium sulfate to sodium Ca–Na–Mg–Cl–SO$_4$
Ca–Mg–Na–SO$_4$–Cl	1.3		
Ca–Na–Cl–SO$_4$	7.9		
Ca–Na–Mg–Cl–SO$_4$	9.2		
Ca–Na–SO$_4$–Cl	2.6		
Mg–Ca–SO$_4$	1.3	8	Magnesium sulfate to calcium Mg–Ca–Cl–SO$_4$
Mg–Na–Ca–SO$_4$–Cl	1.3		
Mg–Na–Cl–SO$_4$	2.6		
Mg–Na–SO$_4$–Cl	2.6		
Na–Ca–Cl–SO$_4$	19.7	70	Chlorinated and sulfated sodium calcium and magnesium with dominance of Na–Ca–Cl–SO$_4$
Na–Ca–Mg–Cl–SO$_4$	9.2		
Na–Ca–Mg–SO$_4$–Cl	6.6		
Na–Ca–SO$_4$–Cl	1.3		
Na–Cl	1.3		
Na–Mg–Ca–Cl	1.3		
Na–Mg–Ca–Cl-SO$_4$	10.5		
Na–Mg–Ca–SO$_4$–Cl	5.3		
Na–Mg–Cl	1.3		
Na–Mg–Cl–SO$_4$	10.5		
Na–Mg–SO$_4$–Cl	1.3		
Na–SO$_4$–Cl	1.3		

Table 3 The Spearman Rank-Order correlation coefficients of the different groundwater parameters

Variables	CE	pH	TDS	Ca	Mg	Na	K	SO$_4$	Cl	HCO$_3$
CE	**1**									
pH	−0.172	**1**								
TDS	**0.963**	**−0.251**	**1**							
Ca	**0.297**	−0.116	**0.431**	**1**						
Mg	**0.523**	−0.080	**0.515**	**−0.306**	**1**					
Na	**0.932**	−0.074	**0.830**	0.096	**0.482**	**1**				
K	**0.794**	−0.138	**0.724**	0.168	**0.382**	**0.766**	**1**			
SO$_4$	**0.543**	0.003	**0.598**	**0.359**	**0.504**	**0.426**	**0.381**	**1**		
Cl	**0.919**	−0.190	**0.848**	**0.232**	**0.363**	**0.908**	**0.729**	**0.305**	**1**	
HCO$_3$	−0.002	−0.092	0.029	0.122	0.047	−0.048	0.060	−0.093	−0.039	**1**

Values in bold are different from 0 with a significance level $\alpha = 0.05$

Agoubi et al. 2012). Hydrogeochemical modeling, as well as statistical and variographic analysis were most used for aquifer investigation and saltwater intrusion. The direct-current resistivity method was also widely used in groundwater investigation and saltwater intrusion due to a rapid advance in microprocessors and numerical modeling techniques (Ahmad et al 1988, Mazac et al 1990; Yang and Lee 2002; Bonomo et al 2002; Kumar et al. 2007; Al-saigh 2010).

In this study, statistical and geostatistical analysis, geochemical modeling and geoelectrical methods were used to investigate groundwater parameters and the main processes controlling groundwater salinity and potential saltwater intrusion in coastal areas of the Marine Jeffara aquifer.

Study area

The study area (Marine Jeffara), located in southeastern Tunisia on the Mediterranean Sea (Fig. 1), is a vast coastal plain characterized by an arid to semi-arid climate. Daily temperatures range from 8 to 45 °C and annual rainfall

varies between 43 and 352 mm, with an annual average of 200 mm (OSS, 2010). Humidity ranges from 43 to 84 % and evaporation rates exceeds 1,700 mm/year. The region is characterized by an intermittent flow regime because of long drought periods and the aforementioned limited surface water resources. Groundwater constitutes the main water resource required to satisfy the different consumption needs of the area (Zouari et al. 2010; Agoubi et al. 2012).
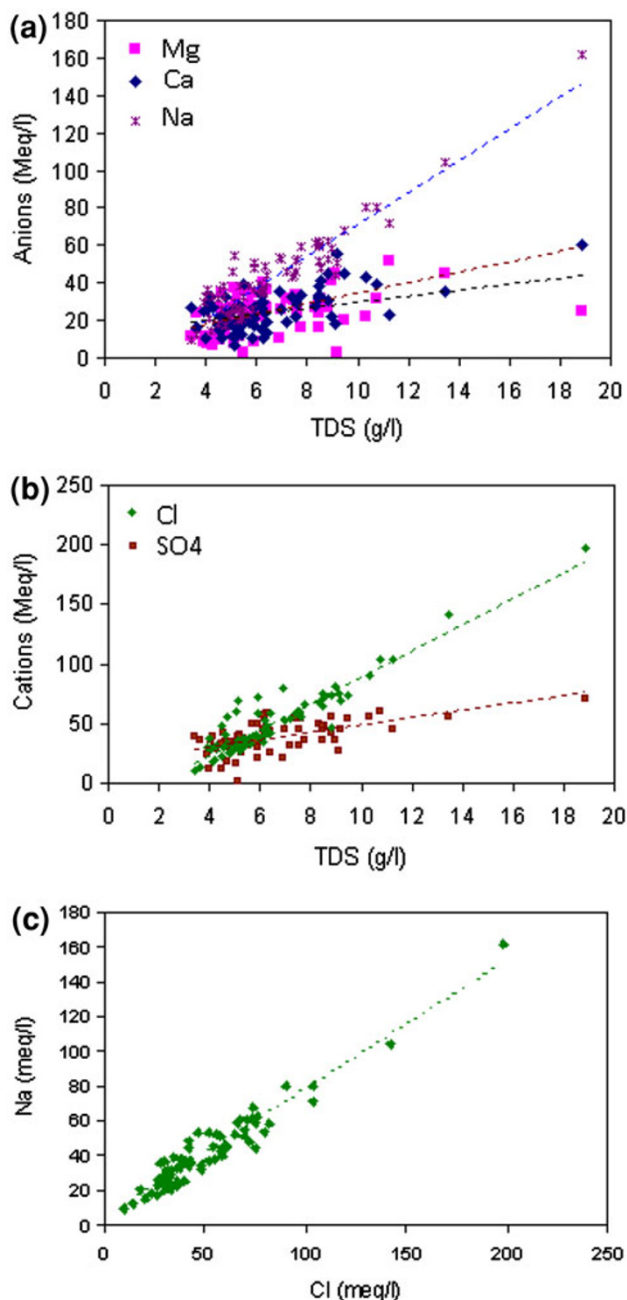
The specific study area is a low-altitude plate (4–35 m) covered by Mio-Plio-quaternary deposits. The overall structure is characterized by faults with small discharges, organized in parallel bands of northwest-southeast orientation (Bouaziz 1995; Jedoui 2000) (Fig. 2). This Mio-Pliocene series fills the Marine Jeffara, whose thickness increases towards the northeast, eventually reaching several hundred meters. The outcrops of these deposits are usually found at the foot of cliffs that border depressions (Agoubi et al. 2012). These deposits come in different facies: red clays, sometimes silty; gypsum crystals that often form the top of the series; fine yellow sand; and conglomerates or sandstone outcrops that often overcome the red clay gypsum.

The Marine Jeffara aquifer is lenticular. Groundwater is housed in the alternations of Mio-Plio-quaternary sand and sandy clays. Its spatial configuration reflects the appearance of horst and graben (Fig. 2). The thickness of the layer increases from west to east and plunges beneath the graben of Ajim, where it exceeds 50 m.

In 1985, the total number of shallow wells was 637, distributed throughout the Marine Jeffara. This number has continued to increase, with 1,365 shallow wells present in 2010 (ODS, 2010). This evolution is mainly due to the expansion of irrigated areas and easy access to these water resources.

Materials and methods

In order to investigate the Marine Jeffara aquifer, a multidisciplinary approach was considered. Geochemical analysis, direct current method as well as statistical and geostatistical techniques were used to identify processes controlling groundwater salinity. Vertical electric sounds (VES) were used to investigate the sub-surface and

Fig. 4 Relationship between TDS and major ions a anions, b cations, and c Na vs Cl
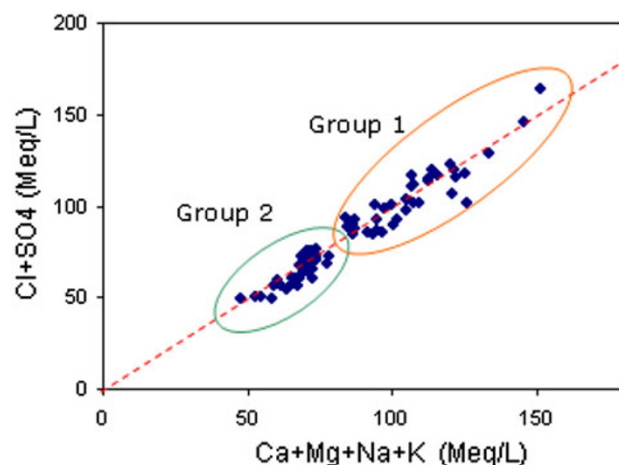
Fig. 5 Relation between $(Ca + Mg + Na + K)$ and $Cl + SO_4$

understand the mechanisms of fault contribution to salt-water intrusion in the shallow aquifer.

Water sampling and chemical analysis

A total of 74 groundwater samples were collected. The physicochemical parameters pH, T (°C), and electric conductivity (EC) were measured in situ using a C933 Multi-Parameter device. Chemical analyses were carried out by ionic chromatography using a Methrohm 850 Professional IC for major ions. Electrical investigation of Jorf shallow aquifer was carried out in July 2010, using GRM 1000 Resistivemeter. The analytical results are summarized in Table 1.

Hydrochemistry

The chemical composition of groundwater is related to the solid product of rock weathering and changes with respect to time and space. Therefore, variation in the concentration levels of different hydrogeochemical constituents dissolved in water determines its usefulness. In this way, Piper and Gibbs diagrams and major ion relationships were established to identify the groundwater mineralization processes.

Statistical and variographic analysis

Hydrochemical data were first statistically analyzed. Multivariate statistical and variographic analyses were preferred for optimal results and reliable interpretations of the results (Banoeng-Yakubo et al. 2008). Hierarchical cluster analysis (HCA) was applied to hydrochemical data to extract the associations corresponding to different processes that control water chemistry. HCA reduces a large number of variables to a small number of principal components (Güler et al. 2002; Hamzaoui-azaza et al. 2009).

Geostatistical tools allow for spatial interpolation and the mapping of spatial variability using the kriging techniques. The theoretical fundamentals of geostatistical methods are described elsewhere (Issaks and Srivastava 1989; Ceron et al. 2000; Sanchez-Martos et al. 2001; Wackernagel 2003). The experimental variogram is the key of any geostatistical analysis as it helps to highlight the spatial correlations between variables. The variogram $\gamma(h)$ is shown in Eq. (1).

$$\gamma(h) = \frac{1}{2N(h)} \sum_{i=1}^{N(h)} \left(Z(x_i) - Z(x_i + h) \right)^2 \tag{1}$$

Where $\gamma(h)$ is the estimated value of the semivariance for lag h; $N(h)$ is the number of experimental pairs separated by vector h, and $Z(x_i)$ and $Z(x_i+h)$ are values of the variable Z at x_i and x_i+h, respectively.

The experimental semivariograms were fitted to various theoretical models generally used in earth sciences, such as spherical, exponential, and Gaussian models (Mehrjardi et al. 2009). The theoretical model yielding the minimum standard error was subsequently chosen for further analysis. Nugget/sill ratio was used to express the extent of spatial autocorrelations of environmental factors. If the ratio is low (<25 %), the variable has strong spatial autocorrelations at a regional scale. A high ratio of nugget effect (>75 %) plays an important role in spatial heterogeneity (Hani and Karimineja 2010).
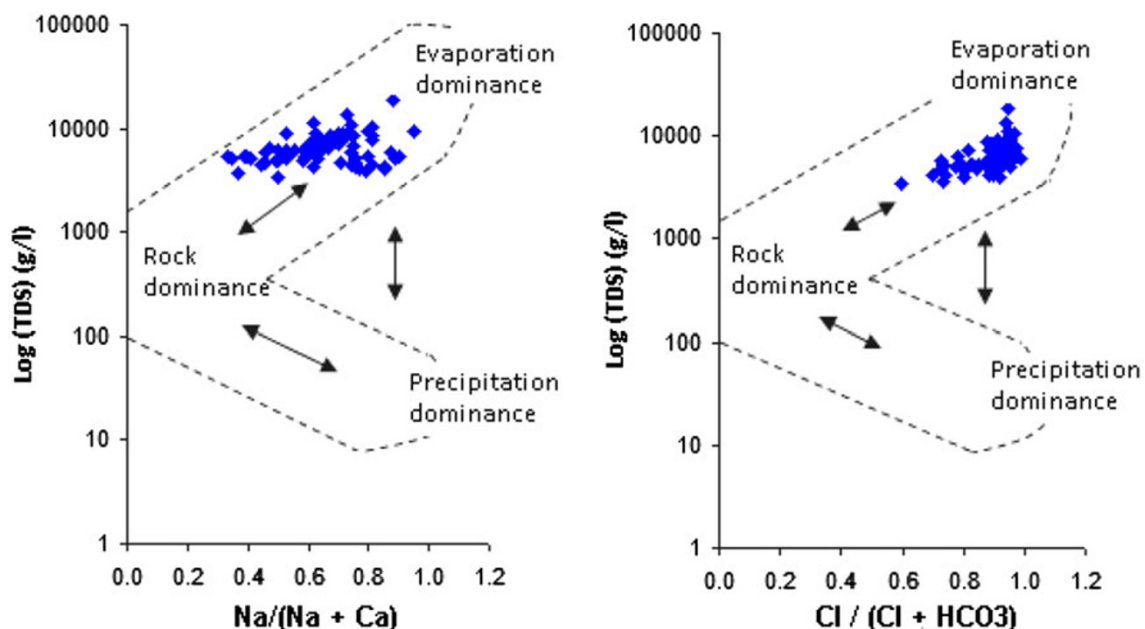

Fig. 6 Gibbs plot indicating the mechanism controlling the groundwater chemistry

Direct current method

Direct current method utilizes four electrodes arranged in a straight line on the ground surface. The Schlumberger array is one of the most commonly used for vertical electrical sounding (VES). Four electrodes (AMNB) are placed along a straight line on the ground surface and the apparent resistivity is computed using Eq. 2.

$$\rho_a = K\frac{\Delta V}{I} \quad \text{with } K = \frac{\left(\frac{AB}{2}\right)^2 - \left(\frac{MN}{2}\right)^2}{MN} \quad (2)$$

where ρ_a is apparent resistivity, AB is current electrodes separation, MN is potential electrodes separation, K is geometric factor, ΔV is potential difference, and I is Current.

The geoelectric survey was carried out using an electrode spacing (AB) of 500 m. The apparent resistivity values were plotted against half the current electrode spacing on a log–log graph. The best fit curves were then traced and the data obtained from the smooth curve were noted. Qualitative and quantitative interpretations of the field curves were carried out using the computer program
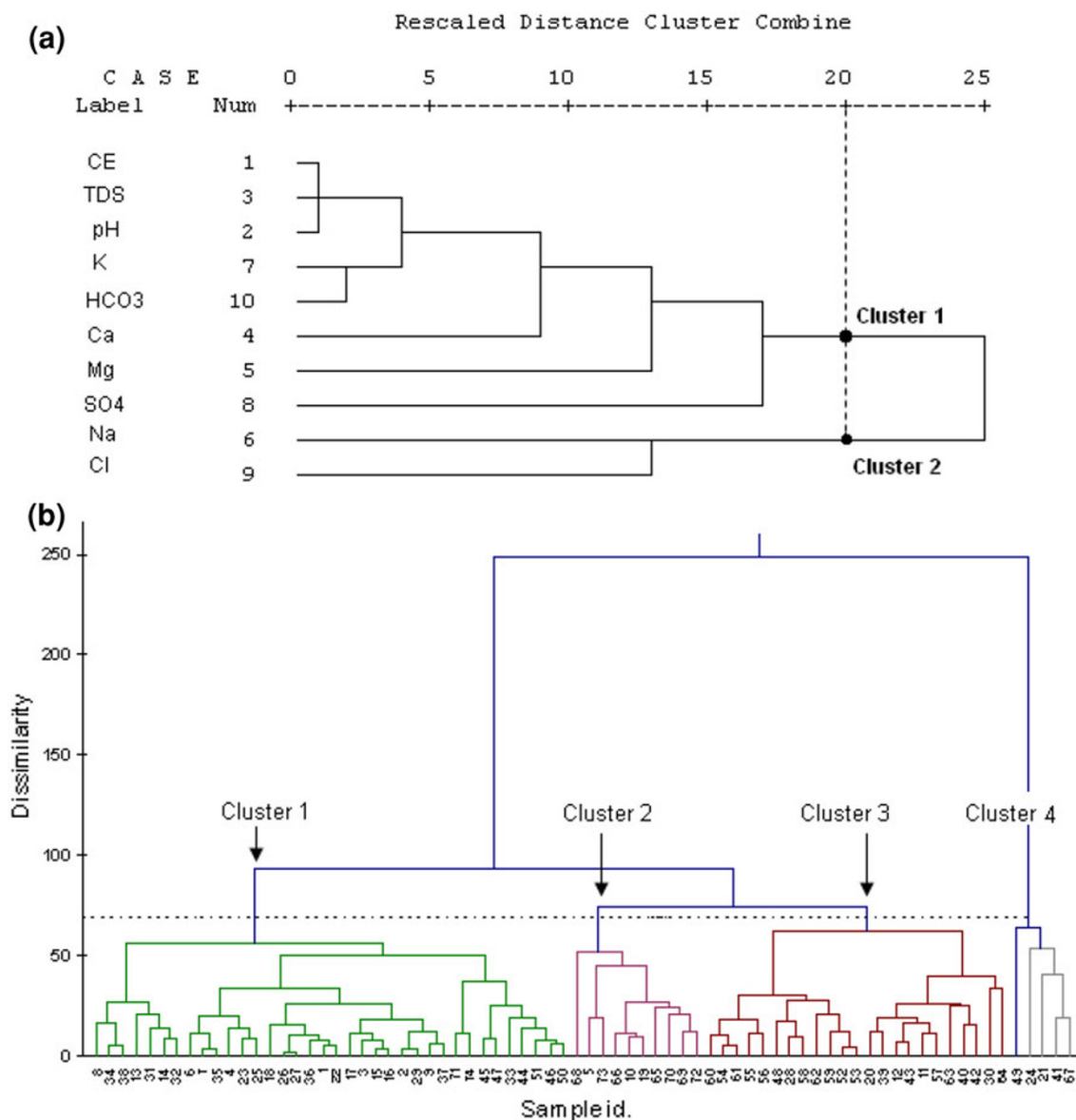

Fig. 7 Groundwater quality dendrogram using average linkage from Q-mode HCA **a** based on environmental parameters and **b** based on groundwater samples

IPI2Win version 3.0.1a developed by Moscow State University (Bobachev 2003).

Results and discussion

Groundwater hydrochemistry

A Piper diagram was used to represent several water samples simultaneously, consisting of two triangles to represent different water facieses. Groundwater samples analyzed data were plotted on the Piper diagram (Fig. 3), using the DIAGRAMS software to identify chemical trends in groundwater (Simler 2009).

These results show a different chemical composition from one area to another, indicating varying sources of mineralization. The abundance of Na and Cl in the Jorf region indicates that potential seawater intrusion may be the region's origin of mineralization. Sodium, chloride, magnesium and sulfate observed in Boughrara region may be related to rock-water interaction causing the dissolution of evaporites (Halite, gypsum and carbonates). The Akara-Zarzis groundwater is dominated by chlorinate, potassium, calcium and sulfate. These facieses indicate that, in addition to the dissolution of carbonates and evaporites, there is also the dissolution of the potassium salt from Sebkhat El Maleh, rich in KCl.

The chemical facies was determined for each well sample with results summarized in Table 2. It was concluded that three main water types dominated. Specifically, 70 % showed facies of chlorinated and sulfated sodium magnesium (Na–Ca–Cl–SO$_4$), 22 % chlorinated facies sulfated sodium to calcium and magnesium (Ca–Na-Mg–Cl–SO$_4$) and 8 % showed a magnesium sulfate facies to calcium (Mg–Ca–Cl–SO$_4$).

Spearman's rank correlation coefficients have been calculated to examine the possible relationships among the measured parameters (Table 3). The TDS concentrations were also plotted as a function of different selected parameters (Fig. 4). High positive correlation was found between TDS and Na$^+$, Cl$^-$, SO$_4^{2-}$, K and Ca^{2+}, which indicates their contribution to groundwater mineralization. Strong correlation between Na and Cl indicates that they must originate from the same source (Fig. 4c). The positive correlation between Ca and SO$_4$ shows the contribution of sulfate and calcium ions to the groundwater mineralization.

The relationship between Cl + SO$_4$ and $\sum$cations (Ca + Mg + Na + K) shows that groundwater was composed of two groups, indicating two water types (Fig. 5). The first group showed a high chloride concentration suggesting saltwater intrusion. However, the second group indicated a low ion concentration, suggesting an interaction of freshwater with rock-water.

These findings suggest that the groundwater from Marine Jeffara has a different chemical composition, which provides information on different processes responsible for its mineralization. The abundance of Cl and Na indicate a local seawater intrusion, while SO$_4$ and Ca ions provide information on water–rock interaction and the dissolution of halite and gypsum.

Hydrochemical data were also plotted on a Gibbs diagram (Fig. 6). Gibbs diagrams suggest that groundwater chemistry is controlled by rock–water interaction and evaporation, which are the dominant factors leading to poor groundwater quality (Gibbs 1970). This is expected, as evaporation greatly

Fig. 8 Hydrochemical composition variable *curves* for groundwater quality
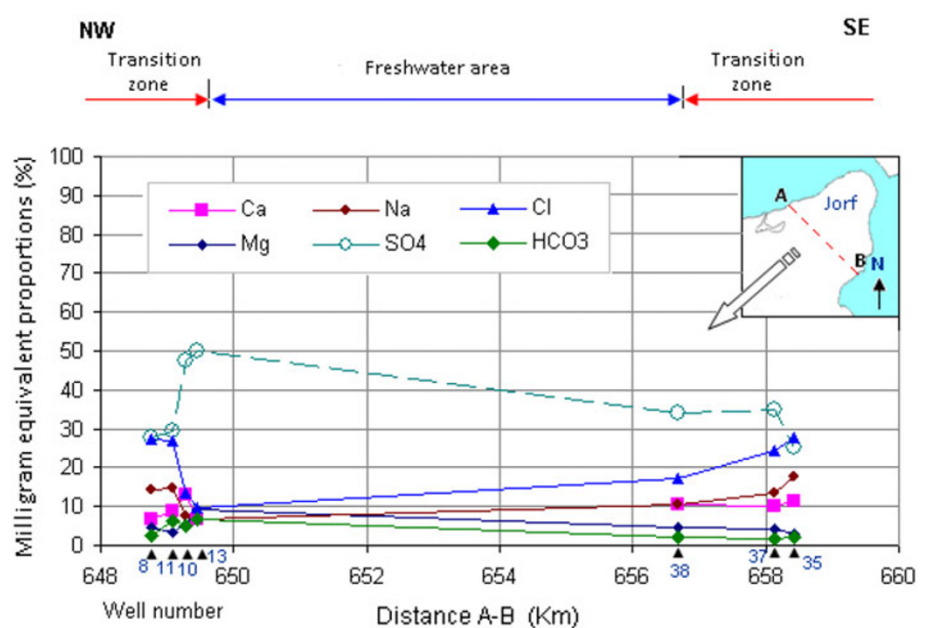
increases the concentrations of ions formed by the chemical weathering of rock, leading to higher salinity (Rao 2002). The effect of climate, evidenced by the influence of evaporation, is another factor to note. High concentrations of calcium and sulfate in groundwater may probably be related to dissolution of gypsum ($CaSO_4.2H_2O$) and anhydrite ($CaSO_4$), while high concentrations of Na and Cl could be related to dissolution of halite).

Cluster analysis was used to determine if the samples could be grouped into statistically distinct hydrochemical groups, potentially resulting in a significant hydrogeologic context. Comparisons based on multiple parameters from different samples were performed and the samples were grouped according to their similarity to each other. Classifications of samples according to their parameters are known as Q-mode classifications. The hierarchical cluster analysis (HCA) resulted in a dendrogram which is a presentation of the groundwater associations in the study area. The Ward's linkage method was used in this analysis. A classification scheme using Euclidean distance for similarity measurement, together with Ward's method for linkage, produces the most distinctive groups. With this classification, each member within the group is more similar to its fellow members than to any member outside
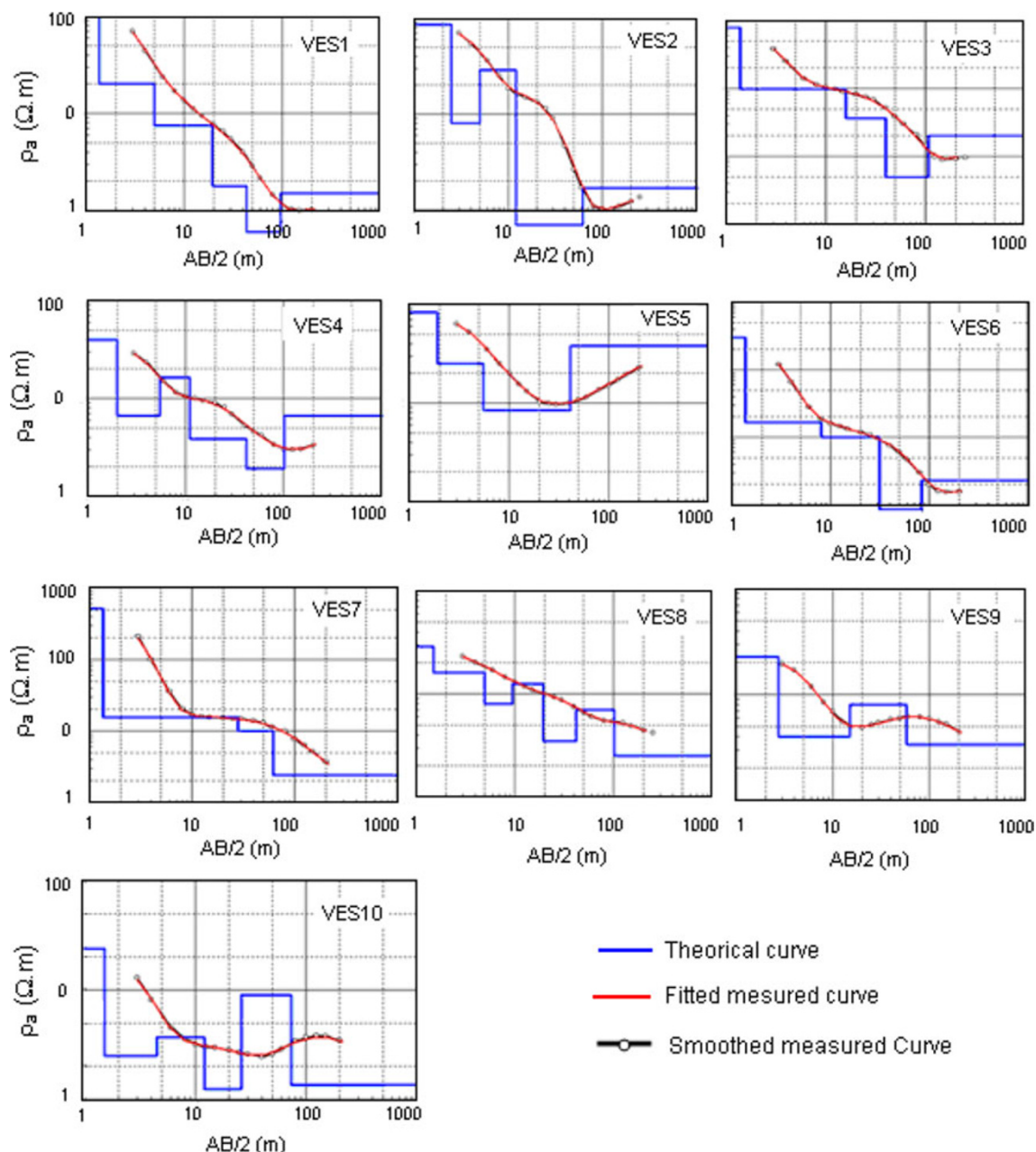

Fig. 9 Model response to experimental apparent resistivity *curves* from VES
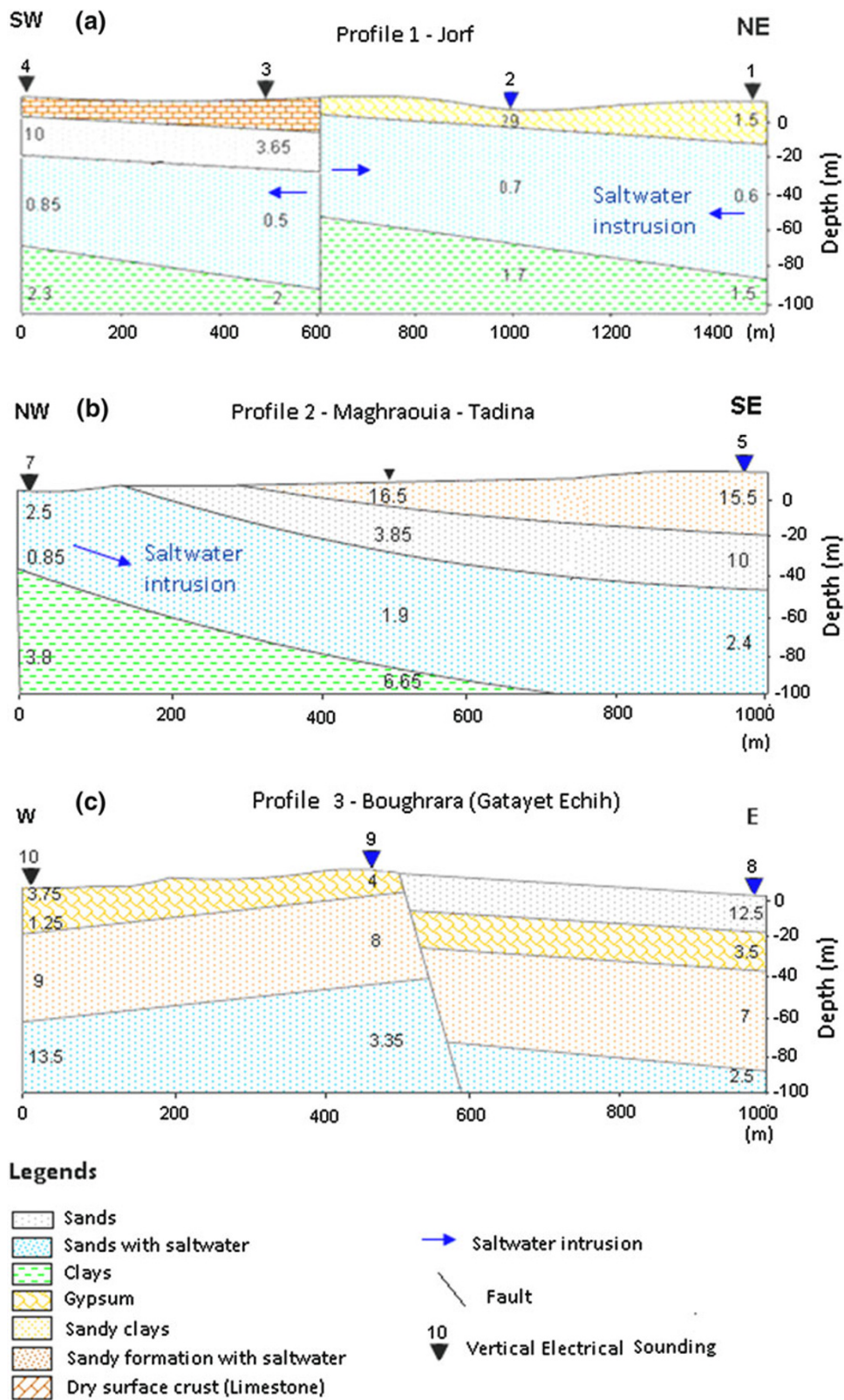
Fig. 10 Cross-section based on geoelectrical model in marine Jeffara

the group (Güler et al. 2002; Belkhiri et al. 2010). Hydrochemical variables measured were utilized in this analysis. Two spatial groundwater types were distinguished from the dendrogram (Fig. 7a). Samples with similar spatial characteristics and relationships were clustered together at low linkage distances, whilst dissimilar samples are clustered at higher linkage distances (Banoeng-Yakubo et al. 2008). The first group represents the SO_4–Ca–Mg–K water. This group is associated with TDS, indicating a contribution of Ca, SO_4, Mg and K to groundwater salinization. The second group indicates a Na–Cl water type, suggesting the dissolution of halite and saltwater intrusion.

The dendrogram of Q-mode HCA was also built on the water samples, showing four main groups of groundwater in Marine Jeffara (Fig. 7b). The cluster differentiation was based on knowledge of geology and groundwater flow patterns as well as geochemical properties in the area (Cloutier et al. 2008). Group 1 is made up of 36 wells, which have moderate salinity and chlorinated and sulfated sodium calcium facies (Cl–SO_4–Na–Ca). Group 2 consists of 10 wells which, located in Akara Peinsula, demonstrate high salinity. Group 3 is made up of 23 wells located in the neighborhood of Sebkhas and indicates a saline water influenced by saline depressions in study area. Finally, Group 4 consists of 5 wells. This group shows the highest salinity (TDS >11 g/l), indicating a Na–Cl water type.

Seawater intrusion

Geochemical evidence

Freshwater from Marine Jeffara aquifer is dominated by chlorinated and sulfated sodium calcium chemical facies. The high concentration of Ca and SO_4 in fresh groundwater in the study area was due to gypsum dissolution contained in mio-plio-quaternary clays. These ions were regarded as original ions characterizing freshwater in the study area. It has been proven that the fresh-salt water interface is not a sudden change boundary surface but a wedge-like transitional zone with its tip on the top between salt and fresh water (Bear et al. 1999; Zhang et al. 2001). During seawater intrusion, SO_4 and Ca concentrations decrease relative to an increase in Cl and Na concentrations. Milligram equivalent proportions of Ca, Na, Cl, Mg, SO_4 and HCO_3 were plotted against the distance from crossing the Jorf Peninsula (Fig. 8). It is interesting to note that the concentration of SO_4 decreases rapidly in the transition zone, which is clearly observable in the northwest part of the peninsula. In the fresh-salt water transitional zone, the concentration of Cl increases rapidly with the development of seawater intrusion. The milligram equivalent proportions of Cl reach 30 % while SO_4 milligram equivalent

proportions decrease from 50 to 30 % (Fig. 8). This results in a relative increase of Na concentration. In the southeast portion of the study area, the transition between freshwater and saltwater is moderate. This can be explained by the influence of the Boughrara lagoon as well as the contributions of the Boughrara fault to groundwater salinization.

Geoelectrical investigation

The model response to experimental apparent resistivity curves from VES and geoelectrical models are shown in Fig. 9. Except for VES 8, all VES show curves with similar trends. Apparent resistivity seems to decrease rapidly with depth, suggesting high water salinity.

Three geoelectrical profiles were created from the 10 VES. The apparent resistivity of vertical profiles was developed and geoectrical cross-sections are presented in Fig. 10. Electric resistivity decreases considerably with depth, indicating high groundwater salinity. The low apparent resistivity ($\rho_a \approx 1$) suggests saltwater mixing. The Maghraouia profile cross-section shows a planar
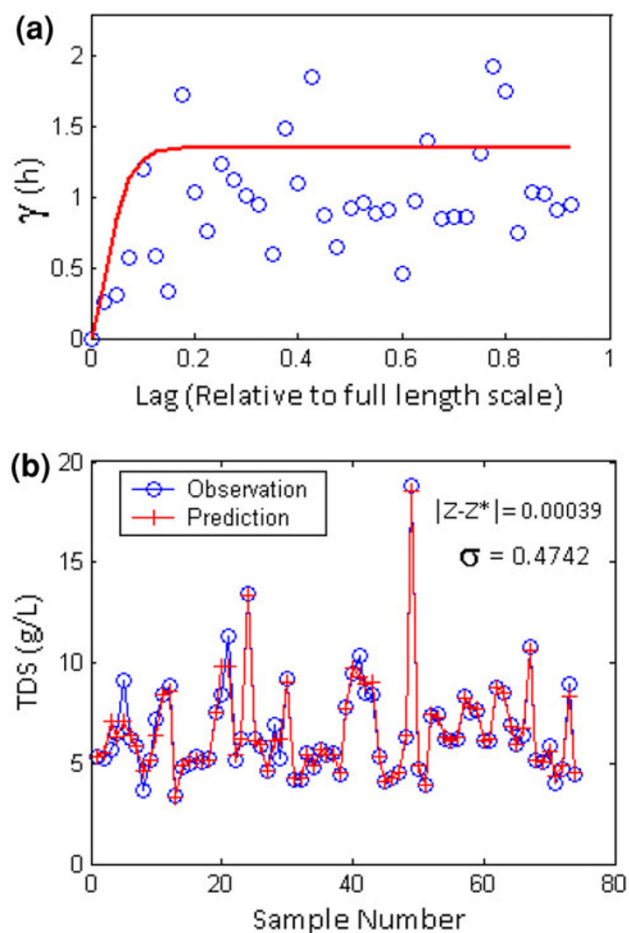

Fig. 11 Experimental semivariogram and cross-validation of TDS

stratification with a low dip to the southeast (Fig. 10b). This cross-section shows a lenticular aquifer consisting of three layers of sand alternating with clay beds. The main aquifer has a depth of 50 m at VES 5. Therefore, the Boughrara profile shows that groundwater mineralization is controlled by rock–water interaction (Fig. 10c).

Total dissolved solids

Geostatistical analysis was performed using EasyKrig MATLAB toolbox (Chu and Hole 2004). The EasyKrig program package uses a graphical user interface (GUI) to simplify the operation. It works in the MATLAB environment and consists of five processing stages: data preparation, semivariogram computation, kriging, visualization, and results saving. A specific advantage of this software is its capability to automatically generate the required default parameters, overcoming the user need to estimate initial parameter values (Chu and Hole 2004; Di Piazza et al. 2009).

In order to map spatial distribution of groundwater salinity, geostatistical analysis was performed. Experimental semivariogram of TDS (Fig. 11) was computed and several models were tested. Root mean squared error (RMSE) was used to select the best fit model. RMSE is often used to compare the performance of interpolation methods (Kitanidis 1997; Kimmeier 2001). RMSE is computed according to Eq. 3, as follows:

$$RMSE = \sqrt{\frac{1}{n}\sum_{i=1}^{n}\left[z(x_i) - z*(x_i)\right]^2} \qquad (3)$$

where $z(x_i)$ is the observed value and $z*(x_i)$ corresponds to the predicted value of observation in location x_i. The smallest value of RMSE is considered the best fit model.

Figure 12 shows higher TDS values along the coast, implying saltwater mixing and the dissolution of gypsum and halite in neighboring areas of Sebkhas. TDS values increase in the central part of Jorf. These findings confirm our hypothesis of various sources of groundwater mineralization in Marine Jeffara. According to these results, it can be concluded that the main process of mineralisation in the study area is seawater intrusion. However, in most parts of the study area, mineral precipitation and the dissolution of halite and gypsum are the most responsible for groundwater mineralization.

Conclusion

The hydrogeochemical parameters of Marine Jeffara aquifer indicated that the groundwater salinity is moderate to high. Three chemical water types of Na–Cl–Mg–Ca–SO$_4$, Ca–SO$_4$–Cl–K–Mg and Ca–SO$_4$–Na–Mg–Cl are recognized
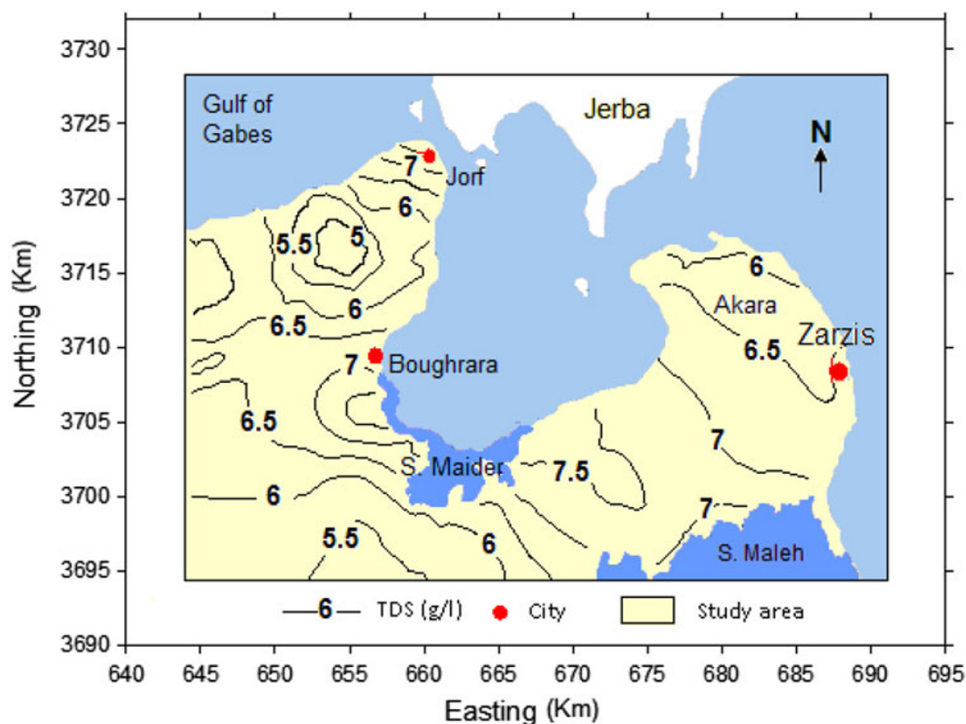

Fig. 12 Kriged map of total dissolved solids (in March 2009)

in the Marine Jeffara groundwater. The Marine Jeffara aquifer is lenticular, formed by alternating layers of sand and sandy clay. The mean aquifer depth of approximately 60 m is most vulnerable to seawater intrusion. Groundwater samples were classified using cluster HCA. Three classes were identified: class 1 indicates a very high saline water with NaCl association; l Class 2 shows a $CaSO_4$ type, indicating rock–water interaction; and Class 3 demonstrates alkalinity in which pH and HCO_3 are associated. Evaporation and rock–water interaction, weathering of evaporates such as gypsum, dissolution of halite and sea water intrusion are the main processes affecting groundwater composition.

References

Agoubi B, Kharroubi A, Abida H (2012) Saltwater intrusion modelling in Jorf coastal aquifer. Geochemical, geoelectrical and geostatistical application Hydrol Process, South-eastern Tunisia. doi:10.1002/hyp.9207

Ahmad S, de Marsily G, Talbot A (1988) Combined use of hydraulic and electrical properties of an aquifer in geostatistical estimation of transmissivity. GroundWater 26(1):78–86

Al-Saigh NH (2010) Geoelectrical detection of subsurface faults at the stern embankment of badoodh reservoir north Iraq. J Appl Sci Environ Sanit 5:65–72

Appelo CAJ, Postma D (2005) Geochemistry, groundwater and pollution, 2nd edn. Balkema, Rotterdam

Banoeng-Yakubo B, Mark Yidana S, Nti E (2008) hydrochemical analysis of groundwater using multivariate statistical methods—the volta region, Ghana KSCE. J Civ Eng 13:55–63

Bear J, Cheng AHD, SorekK S, Ouazar D, Herrera I (1999) Seawater Intrusion in Coastal Aquifers: Concepts. Methods and Practices, Kluwer Academic Publishers, Dordrecht

Belkhiri L, Boudoukha A, Mouni L, Baouz T (2010) Multivariate statistical characterization of groundwater quality in Ain Azel plain, Algeria African. J Environ Sci Technol 4(8):526–534

Bobachev A (2003) IPI2Win–IPI to win. Moscow State University, Resistivity Sounding Interpretation

Bonomo N, Osella A, Martinelli P (2002) Geoelectrical modeling of shallow structures using parallel and perpendicular arrays. Earth Planets Space 54:523–533

Bouaziz S (1995) Etude de la tectonique cassante dans la plateforme et l'atlas sahariens (Tunisie méridionale): évolution des paléo-champs de contrainte et implication géodynamique. Thèse de doctorat es-sciences géologiques, université de Tunis I

Ceron JC, Jimenez-Espinosa R, Pulido-Bosch A (2000) Numerical analysis of hydrochemical data: a case study (Alto Guadalentín, southeast Spain). Appl Geochem 15:1053–1067

Chu D, Hole W (2004) The GLOBEC Kriging Software Package—EasyKrig3.0

Cloutier V, Lefebvre R, Therrien R, Savard MM (2008) Multivariate statistical analysis of geochemical data as indicative of the hydro-geochemical evolution of groundwater in a sedimentary rock aquifer system. Hydrol J 353:294–313

Di Piazza A., Di Piazza MC, Vitale G (2009) A Kriging-based partial shading analysis in a large photovoltaic field for energy forecast.

international conference on renewable energies and power quality (ICREPQ'09) Valencia (Spain), 15th–17th April, 2009

Djabri L, Rouabhia A, Hani Ch, Lamouroux A (2008) Pulido-BoschOrigin of water salinity in a lake and coastal aquifer system. Environ Geol 54:565–573. doi:10.1007/s00254-007-0851-2

Geminez E, Morell I (1997) Hydrogeochemical analysis of salinization processes in the coastal aquifer of oropea (Castellon, Spain). Environ Geol 29:118–131

Gibbs RJ (1970) Mechanisms controlling world water chemistry. Science 17:1088–1090

Güler C, Thyne DG, McCray EJ, Turner AK (2002) Evaluation of graphical and multivariate statistical methods for classification of water data. Hydrogeol J 10:455–474

Hamzaoui-Azaza F, Bouhlila R, Gueddari M (2009) Geochemistry of fluoride and major ion in the groundwater samples of triassic aquifer (South Eastern Tunisia), through multivariate and hydrochemical techniques. J App Sci Res 5(11):1941–1951

Hani A, Karimineja MT (2010) Toxic metal distribution in Soils of Kaveh Industrial city Iran. World Appl Sci J 8(11):1333–1342

Issaks E, Srivastava R (1989) Applied Geostatistics. Oxford University Press, New York

Jedoui Y (2000) Sédimentologie et géochronologie des dépôts littoraux quaternaires: reconstitution des variations des paléoclimats et du niveau marin dans le sud est tunisien. Thèse de doctorat es-sciences géologiques, université de Tunis II

Kimmeier F (2001) 3-D groundwater flow modelling in heterogenous geologic media: integrated approach using spatial and temporal database, geostatistic and GIS. PhD thesis, Centre d'hydrogéologie de Neuchtal, Suisse

Kitanidis PK (1997) Introduction to geostatistics. Application in Hydrogeology, Cambridge Univ Press, Cambridge

Kumar D, Ahmed S, Krishnamurthy NS, Dewandel B (2007) Reducing ambiguities in vertical electrical sounding inter pretations: a geostatistical application. J Appl Geophys 62:16–32

Mahesha A, Nagaraja SH (1996) Effect of natural recharge on seawater intrusion in coastal aquifer. J Hydrol 174:211–220

Mazac O, Cislerova M, Kelly WE, Landa I, Venhodova D (1990) Determination of hydraulic conductivities by surface geoelectrical methods. In S.H. Ward (ed). "Geotechnical and environmental geophysics V.2. Environ Groundwater Appl 125:125–131

Mehrjardi RT, Johromi MZ, Mahmodi M, Heidari A (2009) Spatial distribution of groundwater quality with geostatics (case study: yazd-Ardakan Plain). World Appl Sci J 4(1):09–17

Mekrazi OF (1974) Etude sommaire de la nappe Mio-Pliocène de la presqu'ile de Jorf (DRE). Rapport DGRE Gabès

Pazand K, Hezarkhani A (2012) Investigation of hydrochemical characteristics of groundwater in the Bukan basin, Northwest of Iran. Appl Water Sci 2:309–315

Rao NS (2002) Geochemistry of groundwater in parts of Guntur district, Andhra Pradesh, India. J Environ geol 41:552–562

Reddy AGS, Reddy DV, Rao PN, Maruthy Prasad K (2010) Hydrogeochemical characterization of fluoride rich groundwater of Wailpalli watershed, Nalgonda District, Andhra Pradesh, India. Environ Monit Assess 171:561–577. doi:10.1007/s10661-009-1300-3

Sanchez-Martos F, Jiménez-Espinosa R, Pulido-Bosch A (2001) Mapping groundwater quality variables using PCA and geostatistics: a case study of Bajo Andarax, southeastern Spain. Hydrol Sci J des Sci Hydrol 46(2):543–555

Simler R (2009) DIAGRAMMES : Logiciel d'hydrochimie multilangage en distribution libre. Laboratoire d'Hydrogéologie d'Avignon, France

Thilagavathi R, Chidambaram SM, Prasanna M, Thivya V, Singaraja C (2012) A study on groundwater geochemistry and water quality in layered aquifers system of Pondicherry region, southeast India. Appl Water Sci 2:253–269

Wackernagel H (2003) Multivariate geostatistics. An introduction with applications, 3rd edn. Springer Berlin

Yang CH, Lee WF (2002) Using Direct current resistivity sounding and geostatistics to aid in hydrogeological studies in the Choshuichi alluvial fan Taiwan. Groundwater 40:165–173

Zhang Z, Jiang L, Yang L, QI Y (2001) Ground water hydrochemical characteristics: seawater intruded area in eastern and southern coast of Laizhou Bay. J Geogr Sci 11(3):350–355

Zouari K, Trabelsi R, Chkir N (2010) Using geochemical indicators to investigate groundwater mixing and residence time in the aquifer system of Djeffara of Medenine (southeastern Tunisia). Hydrogeol J 19:209–219. doi:10.1007/s10040-010-0673-2